

See discussions, stats, and author profiles for this publication at: <https://www.researchgate.net/publication/260643002>

# Electronegativity Estimator Built on QTAIM-Based Domains of the Bond Electron Density

ARTICLE in JOURNAL OF COMPUTATIONAL CHEMISTRY · MAY 2014

Impact Factor: 3.59 · DOI: 10.1002/jcc.23574

---

CITATIONS

4

---

READS

33

3 AUTHORS, INCLUDING:



[David Ferro-Costas](#)

University of Vigo

13 PUBLICATIONS 33 CITATIONS

SEE PROFILE



[Ricardo Mosquera](#)

University of Vigo

144 PUBLICATIONS 1,812 CITATIONS

SEE PROFILE

# Electronegativity Estimator Built on QTAIM-Based Domains of the Bond Electron Density

David Ferro-Costas, Ignacio Pérez-Juste, and Ricardo A. Mosquera\*

The electron localization function, natural localized molecular orbitals, and the quantum theory of atoms in molecules have been used all together to analyze the bond electron density (BED) distribution of different hydrogen-containing compounds through the definition of atomic contributions to the bonding regions. A function,  $g_{A|H}$ , obtained from those contributions is analyzed along the second and third periods of the periodic table. It exhibits periodic trends typically assigned to the electronegativity

( $\chi$ ), and it is also sensitive to hybridization variations. This function also shows an interesting S shape with different  $\chi$ -scales, Allred–Rochow's being the one exhibiting the best monotonical increase with regard to the BED taken by each atom of the bond. Therefore, we think this  $\chi$  can be actually related to the BED distribution. © 2014 Wiley Periodicals, Inc.

DOI: 10.1002/jcc.23574

## Introduction

Electronegativity ( $\chi$ ) is one of the most important and useful concepts within chemistry. Lots of definitions can be found for it, from the one found in the IUPAC Gold Book<sup>[1]</sup> (*the power of an atom to attract electrons to itself*) to those found in books of general chemistry (as, e.g., “the ability of an atom to attract toward itself the electrons in a chemical bond,” given by Chang; or “an atom's ability to compete for electrons with other atoms to which it is bonded,” given by Petrucci et al.).<sup>[2,3]</sup> Despite the immensity of possible definitions that can be found, all of them give rise to the same idea: the comparison between  $\chi_A$  and  $\chi_B$  is somehow a measure of how much of the A–B bond electron density (BED) is taken by (or attracted to) each of the atoms involved in it.

Different scales of  $\chi$  were proposed throughout the years, Pauling<sup>[4]</sup> being one of the first to provide a fully quantified scale for its measurement [Pauling's Electronegativity (PE)], on the basis of thermal data interpreted through simple quantum mechanical arguments.<sup>[a]</sup> In his scale, the difference of electronegativity between two atoms, A and B ( $\chi_A - \chi_B = \chi_A^B$ ), depends on the difference between the bond energy of the A–B bond,  $E_{AB}^b$ , and that predicted from additivity considering A–A and B–B covalent bonds,  $(E_{AA}^b + E_{BB}^b)/2$ , as indicated in eq. (1) (bond energies in eV). Usually, the value for H ( $\chi_H = 2.20$ , given by Huggins in 1953)<sup>[9]</sup> is assigned as the basis of the scale of relative electronegativities.<sup>[10]</sup>

$$(\chi_A - \chi_B)^2 = \left[ E_{AB}^b - \frac{E_{AA}^b + E_{BB}^b}{2} \right] \quad (1)$$

Together with PE, other two scales are of great popularity: Mulliken's and Allred–Rochow's electronegativities (ME and A-RE, respectively). On one hand, Mulliken<sup>[11]</sup> proposed the arithmetic

mean of the ionization potential (IP) and the electron affinity (EA), eq. (2), as a good measure of the ability of an atom to attract electrons to itself. As Mulliken did, it is of importance to point that these two magnitudes are not those of the ground state of the atom, but those of the valence state. According to this definition, an electronegativity value can be given to an atom depending on the valence state it assumes in a molecule.

$$\chi_A = \frac{IP_A + EA_A}{2} \quad (2)$$

Conversely, Allred and Rochow related  $\chi$  to the force of attraction between a nucleus and an electron from a bonded atom,<sup>[12]</sup> through the use of the effective nuclear charge ( $Z_{\text{eff}}$ ) experienced by valence electrons, and the covalent radius,  $r_{\text{cov}}$ , as shown in eq. (3) ( $r_{\text{cov}}$  in Å).

$$\chi_A = 0.359 \cdot \frac{Z_{\text{eff}}}{r_{\text{cov}}^2} + 0.744 \quad (3)$$

It is remarkable that, within the framework of the conceptual density functional theory (DFT),<sup>[13]</sup> Mulliken's electronegativity arises as a finite-difference approximation<sup>[14]</sup> of the definition given by Iczkowski and Margrave,<sup>[15]</sup> shown in eq. (4), where  $E$  is the energy of the system,  $N$  is the total number of electrons, and  $v$  is the external potential. However, this electronegativity differs from the original given by Mulliken because, as it is restricted to the ground states, it only involves the IP and the EA of ground state atoms.

This article was published online on 9 March 2014. An error was subsequently identified. This notice is included in the online and print versions to indicate that both have been corrected on 24 March 2014.

D. Ferro-Costas, I. Pérez-Juste, R. A. Mosquera  
Departamento de Química Física, Universidade de Vigo, Facultade de  
Química, Lagoas-Marcosende s/n, 36310, Vigo, Galicia, Spain  
E-mail: mosquera@uvigo.es

Contract/grant sponsor: Spanish Ministry of Economy; contract/grant number: CTQ2010-21500

© 2014 Wiley Periodicals, Inc.

<sup>[a]</sup>Contrary to popular belief, there are two scales of electronegativities<sup>[5]</sup> preceding Pauling's one: the V/S scale<sup>[6,7]</sup> of Worth Rodebush and the Ionic Potential scale<sup>[8]</sup> of Groves Cartledge.

$$\chi = - \left( \frac{\partial E}{\partial N} \right)_v \quad (4)$$

From a chemical point of view, Mulliken's original definition based on the valence states of the atom is more versatile, as it allows obtaining diverse electronegativity values for the same atom, reflecting the effect of different chemical surroundings. This versatility can be also obtained through the definition of the orbital electronegativity for the atomic orbital  $i$ .<sup>[16]</sup> This is done by replacing the total number of electrons by the corresponding orbital occupation number  $N_i$  in eq. (4). Particularly, the electronegativity considering a single occupied atomic orbital  $i$  is obtained using the IP and the EA of the corresponding orbital,  $IP_i$  and  $EA_i$ , in eq. (2). This magnitude is introduced as a measure of the potential of the orbital to attract and to withhold electrons.<sup>[17]</sup> Thus, the use of hybrid orbitals could be intuitively equivalent to the consideration of valence states in the original ME.

We want to highlight that the scales previously introduced here are, basically, based on energetic considerations and none of them is directly related to the amount of BED belonging to a certain atom. As a consequence, the relationship between electronegativity difference and BED distribution could be actually considered imprecise.

In this work, we explore two possible ways to measure directly the ability of an atom to attract the BDE to itself and, as a consequence, to check if  $\chi_A^B$  is physically related to the BED distribution. For such a purpose, we make use of a partitioning scheme of the three-dimensional space using a combination of both electron localization function (ELF)<sup>[18,19]</sup> and quantum theory of atoms in molecules (QTAIM)<sup>[20,21]</sup> basins, presented in a recent work.<sup>[22]</sup> Furthermore, we also use a scheme based on natural localized molecular orbitals (NLMOs)<sup>[23]</sup> and QTAIM. We think that the use of both schemes could supply pertinent data to assess if electronegativities and BED are actually related.

It is noteworthy that a similar attempt was performed in the framework of the natural bond orbital (NBO) theory by Weinhold and Landis,<sup>[24]</sup> through the definition of their ionicity parameter for the A–B bond,  $i_{AB}$ .<sup>[25]</sup> This parameter is said to measure the polarity of the  $\sigma_{AB}$  NBO bond and it has been nicely related to the electronegativity difference between A and B.

## Electronegativity and Electron Populations

### Topological partition and ELF $\cap$ QTAIM scheme

Mathematically, the vector field of a scalar function  $h: \mathbb{R}^3 \rightarrow \mathbb{R}$  can be used to split its domain ( $\mathbb{R}^3$ ) into basins of attraction by following the trajectory of  $\nabla h(\mathbf{r})$  for each point of  $\mathbb{R}^3$ . The surface around an attractor displaying a zero flux in the gradient vector of the scalar function, eq. (5), defines the limits (separatrix) of the basin for the attractor. In this manner,  $h$  gets rise to a disjoint and complete division of the  $\mathbb{R}^3$  domain into a set of  $h$ -basins limited by the condition shown in eq. (5), where  $\mathbf{n}(\mathbf{r})$  is the normal vector to the surface  $S$ .

$$\nabla h(\mathbf{r}) \cdot \mathbf{n}(\mathbf{r}) = 0 \quad \forall \mathbf{r} \in S \rightarrow \int_S \nabla h(\mathbf{r}) \cdot \mathbf{n}(\mathbf{r}) ds = 0 \quad (5)$$

The QTAIM provides a partition of  $\mathbb{R}^3$  with physical significance, obtained after the generalization of the action principle

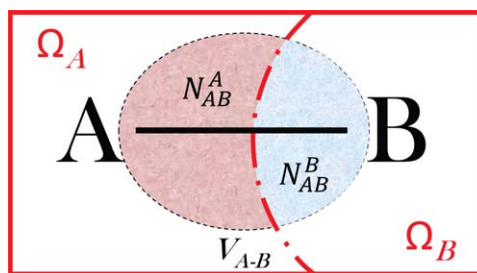


Figure 1. Scheme of the QTAIM contributions to the disynaptic A–B basin, eq. (7). For the sake of simplicity, the magnitudes  $N(V_{A-B})$  and  $N(V_{A-B} \cap \Omega_k)$  are written as  $N_{AB}$  and  $N_{AB}^k$ , respectively.

to a subsystem of some total system.<sup>[26]</sup> In this case, the  $h$  scalar function is the electron density  $\rho$  and its attraction basins are identified with atoms in the molecule. These basins, normally designed by  $\Omega$ , are called atomic basins within the QTAIM framework. It is really of importance to remark that this division (with  $h=\rho$ ) arises from the laws of quantum mechanics and, therefore, eq. (5) is not the only simple topological condition in this situation.

Conversely, when the ELF<sup>[18]\*</sup> is used as  $h$ , basins usually associated to regions with different pairs of electrons in a molecule are obtained. In general, these basins are classified as core (containing a nucleus different from H) and valence basins (without nucleus or with a H one). The last ones are also defined through their synaptic order: monosynaptic ( $V_A$ , representing an A lone pair of electrons), disynaptic ( $V_{A-B}$ , bond between A and B atoms) and so forth.

As both QTAIM and ELF partitions are disjoint and complete, their superposition leads to the definition of regions with chemical significance within atomic domains (and, similarly, to atomic regions inside ELF basins). As a result, the electron population of a  $V_{A-B}$  bond basin ( $N_{AB}$ ) can be expressed by atomic contributions, as shown in eq. (6),  $M$  being the number of atomic basins.<sup>†</sup> In simple cases, eq. (6) can be reduced to eq. (7) (a simple scheme is shown in Fig. 1) with almost negligible error, as confirmed in a previous work.<sup>[22]</sup>

$$N_{AB} = N(V_{A-B} \cap [\Omega_1 \cup \dots \cup \Omega_k \cup \dots \cup \Omega_M]) = \sum_{k=1}^M N_{AB}^k \quad (6)$$

$$N_{AB} \cong N_{AB}^A + N_{AB}^B = N_{AB}^{A \cup B} \quad (7)$$

### NLMO $\cap$ QTAIM scheme

NLMO procedure is a direct extension of the NBO method.<sup>[24]</sup> Each NLMO closely resembles a parent NBO and, unlike the latter, they are a valid solution of the Hartree–Fock equations.

\*The ELF function is defined as  $\eta(\mathbf{r}) = [1 + (D_\sigma(\mathbf{r})/D_\sigma^0(\mathbf{r}))^2]^{-1}$ , where  $D_\sigma$  is the Laplacian of the conditional pair probability calculated from a single determinantal wave function and  $D_\sigma^0$  corresponds to a uniform electron gas with spin-density equal to the local value.

<sup>†</sup>For the sake of simplicity, the magnitudes  $N(V_{A-B})$  and  $N(V_{A-B} \cap \Omega_k)$  are written as  $N_{AB}$  and  $N_{AB}^k$ , respectively.

Moreover, as they are also natural molecular orbitals (i.e., they diagonalize the first-order reduced density matrix).<sup>‡</sup> NLMOs provide a partition of the electron density of the system,  $\rho(\mathbf{r})$ , in terms of pairs-of-electrons densities with chemical significance, as shown in eq. (8). In it,  $\phi_i^{\text{loc}}$  represents the  $i$ th occupied NLMO, whereas  $\rho_i$  is the electron density of this orbital, which integrates to its occupation number,  $N_i$ .

$$\rho(\mathbf{r}) = \sum_i^{\text{occ}} N_i |\phi_i^{\text{loc}}(\mathbf{r})|^2 = \sum_i^{\text{occ}} \rho_i(\mathbf{r}) \quad (8)$$

On the other side, as NLMOs are said to adopt the bonding pattern of a localized Lewis structure, they can be used to represent core, bonds, lone pairs and so forth. Thus, although NLMO and ELF partitions of  $\rho(\mathbf{r})$  display a different nature (fuzzy vs. disjoint, respectively), they are two sides of the same coin: both describe different “chemical regions” of the molecule.

Let us now consider an A—B bond characterized by the  $\phi_{\text{AB}}^{\text{loc}}$  orbital. As this orbital is basically localized between A and B nuclei, its electron population (two electrons when dealing with monodeterminantal wave functions in closed-shell systems) is mainly recovered when integrating in the  $\Omega_A \cup \Omega_B$  region. In this situation, the approximation shown in eq. (9), where  $N_{\text{AB}}^{\text{A}}$  represents the A-atomic contribution of  $N_{\text{AB}}$  anew, is fulfilled.

$$N_{\text{AB}} = \int \rho_{\text{AB}} d\mathbf{r} \cong \int_{\Omega_A \cup \Omega_B} N_{\text{AB}} |\phi_{\text{AB}}^{\text{loc}}|^2 d\mathbf{r} = N_{\text{AB}}^{\text{AUB}} = N_{\text{AB}}^{\text{A}} + N_{\text{AB}}^{\text{B}} \quad (9)$$

### Electronegativity and the $g_{\text{AB}}$ index

Let us consider a bond between atoms A and B (described through an ELF basin or a NLMO). In general, as indicated in previous sections, the bond regions can be described through two QTAIM contributions: one for each atom of the bond [eqs. (7) and (9)]. When both atoms have the same electronegativity, both QTAIM contributions are expected to be equal. This is,  $N_{\text{AB}}^{\text{A}} = N_{\text{AB}}^{\text{B}} = N_{\text{AB}}^{\text{AUB}}/2$ . However, the electronegativity difference between them ( $\chi_{\text{A}}^{\text{B}} = \chi_{\text{A}} - \chi_{\text{B}}$ ) is said to cause a nonhomogeneous distribution of the BED, so that there is a variation of electron population ( $\Delta N_{\text{AB}}$ ) with regard to the system with  $\chi_{\text{A}}^{\text{B}} = 0$ . Therefore,  $N_{\text{AB}}^{\text{A}}$  will be given by eq. (10), where a minus sign would replace the plus one for  $N_{\text{AB}}^{\text{B}}$ .

$$N_{\text{AB}}^{\text{A}} = \frac{N_{\text{AB}}^{\text{AUB}}}{2} + \Delta N_{\text{AB}} \quad (10)$$

If it is, indeed, possible to define a magnitude for atoms that can be used in molecules to get knowledge about how the BDE is distributed (i.e., basically, what we expect from the electronegativity),  $\Delta N_{\text{AB}}$  should depend, then, on  $\chi_{\text{A}}^{\text{B}}$ . Taking into account eq. (10) and that  $N_{\text{AB}}^{\text{A}} \in [0, N_{\text{AB}}^{\text{AUB}}]$ , an adimen-

sional quantity restricted to the  $[-1, +1]$  interval, hereafter called  $g_{\text{AB}}$  index, can be defined:

$$g_{\text{AB}} = \frac{2\Delta N_{\text{AB}}}{N_{\text{AB}}^{\text{AUB}}} = \frac{N_{\text{AB}}^{\text{A}} - N_{\text{AB}}^{\text{B}}}{N_{\text{AB}}^{\text{A}} + N_{\text{AB}}^{\text{B}}} \quad (11)$$

This index inherits the  $\Delta N_{\text{AB}}$  dependence on  $\chi_{\text{A}}^{\text{B}}$  and, although we ignore the analytical form of  $g_{\text{AB}}$  in terms of  $\chi_{\text{A}}^{\text{B}}$ , its value should increase monotonically with it. The obvious problem here is that these electronegativities, if they really exist, are unknown. However, if others (e.g., Pauling's one) possess the intrinsic ability to describe the BED distribution, a relationship with  $g_{\text{AB}}$  should be found.

### Hydrogen compounds as a reference: the $g_{\text{AH}}$ index

As stated above, H is the arbitrary reference in some electronegativity scales (as in Pauling's one). Thus, it is (at least) tempting to use hydrogen compounds to check the relation between electronegativity scales and the BED distribution indicated by the  $g_{\text{AB}}$  index (with B = H). Therefore, closed-shell hydrogen compounds ( $\text{AH}_n$ ) have been used to get  $g_{\text{AH}}$  for second and third period elements.

As we checked in other work,<sup>[22]</sup> QTAIM hydrogen basins are, in general, contained within ELF disynaptic A—H basins ( $\Omega_{\text{H}} \subset V_{\text{A-H}}$ ). In the same vein, the electron density inside the hydrogen atomic basin is mostly described by the A—H bond NLMO. As a direct consequence,  $N_{\text{A-H}}^{\text{H}} \simeq N_{\text{H}}$  in both ELF  $\cap$  QTAIM and NLMO  $\cap$  QTAIM schemes, this approximation being more accurate in the first case.<sup>§</sup> With this in mind, it is straightforward to obtain the approximated relationship between  $g_{\text{AH}}$  and the QTAIM atomic charge of hydrogen ( $q_{\text{H}}$ ) shown in eq. (12), where  $\Delta_{\text{AH}}$  is given by eq. (13).

$$g_{\text{AH}} \cong (1 - N_{\text{H}}) + N_{\text{H}} \left( 1 - \frac{2}{N_{\text{AH}}^{\text{AUB}}} \right) = q_{\text{H}} - \Delta_{\text{AH}} \quad (12)$$

$$\Delta_{\text{AH}} = \frac{N_{\text{H}}}{N_{\text{AH}}^{\text{AUB}}} (2 - N_{\text{AH}}^{\text{AUB}}) \quad (13)$$

If  $\Delta_{\text{AH}}$  is close to zero, it can be also stated that  $g_{\text{AH}} \simeq q_{\text{H}}$ . This situation is achieved when: (i) the A—H BED mostly belongs to A (this is,  $N_{\text{H}}/N_{\text{AH}}^{\text{AUB}}$  close to zero), what should happen when A is a very electronegative atom; and/or (ii) the A—H BED population contained within A and H atoms is close to two electrons. In general, one or both conditions are nearly fulfilled for both schemes and replacing the  $g_{\text{AH}}$  index by the atomic charge of the hydrogen could be taken as a low computational-cost approach. From this point of view, the  $g_{\text{AH}}$  index recalls in behavior the NBO ionicity for hydrogen compounds ( $i_{\text{AH}}$ ),<sup>[25]</sup> which is basically equal to the hydrogen NBO charge. Thus, the difference between  $g_{\text{AH}}$  and  $i_{\text{AH}}$  would be, basically, given by the one between QTAIM and NBO hydrogen

<sup>§</sup>For ELF  $\cap$  QTAIM, the difference between  $N_{\text{H}}$  and  $N_{\text{A-H}}^{\text{H}}$  is smaller than 0.1%, excluding particular cases (F and Si with HF/6-31G) where the small size of the basis set produces a spurious ELF basin inside the QTAIM hydrogen. For NLMO  $\cap$  QTAIM, the relative differences are larger, reaching 11% in some cases.

<sup>‡</sup>This is true in monodeterminantal wave functions. When dealing with post-HF wave functions (as CI ones), NLMOs are not natural molecular orbitals.

populations. In this point, it has to be stressed that, in general, approximating  $g_{AB}$  by  $q_B$  does not hold when B is involved in more than one bond.

In the low computational-cost approach, both  $\text{ELF} \cap \text{QTAIM}$  and  $\text{NLMO} \cap \text{QTAIM}$  are reduced to the same scheme (obtaining  $q_H$  with QTAIM). However, we consider worthy the effort involved in eq. (11) for both analysis, not only to prevent the effects introduced by the large number of approximations but also to check up the different descriptions of bonding regions given by ELF and NLMOs methodologies. In fact,  $\Delta_{AH}$  values can be as large as 0.19 and 0.09 au for  $\text{ELF} \cap \text{QTAIM}$  and  $\text{NLMO} \cap \text{QTAIM}$ , respectively. Thus, although the trends shown by  $g_{AH}$  and  $q_H$  are similar, this approximation can introduce important relative errors in the determination of the actual value of  $g_{AH}$ .

## Computational Details

### Computation of $N_{AB}^A$ and $N_{AB}^B$ values in both schemes

As indicated in a previous work,<sup>[22]</sup> QTAIM and ELF basins were obtained using the near-grid method with boundary refinement step<sup>[27]</sup> through the Multiwfn software.<sup>[28]</sup> For each hydrogen compound ( $AH_n$ , A being the central atom of which we want to know  $g_{AH}$ ), all its QTAIM or ELF basins present the same grid of points, centered (in general) in the A atom. The standard grid used is a  $15 \times 15 \times 15$  bohr<sup>3</sup> cube, with a grid spacing in each axis of 0.02 bohr (grid parameters used in each system is shown in the Supporting Information). Each basin is defined by a value of 1 or 0 in every point, depending on whether or not the point belongs to the basin. Therefore, each basin is basically characterized by a 0/1 array. The product of its value for the  $\Omega$  basin by the one for the  $i$ th ELF basin ( $C_i$ ) at a certain point indicates if it belongs (1) or not (0) to the  $C_i \cap \Omega$  region, ending up in the definition of a new 0/1 vector for that region.

The population of every  $C_i \cap \Omega$  fragment was carried out by elementary numerical integration of the electron density, as shown in eq. (14), where  $V_k$  is the volume associated to the  $k$ th point of the grid (composed by a number of points equal to  $np$ ),  $\bar{\rho}(\mathbf{r}_k)$  is the averaged value of the electron density<sup>††</sup> at  $\mathbf{r}_k$ , and  $(\mathbf{0}/\mathbf{1})_k^{i,\Omega}$  is the 0/1 vector, which defines whether or not the  $k$ th point belongs to  $C_i \cap \Omega$ .

$$N(C_i \cap \Omega) \cong \sum_{k=1}^{np} (\mathbf{0}/\mathbf{1})_k^{i,\Omega} \cdot \bar{\rho}(\mathbf{r}_k) \cdot V_k \quad (14)$$

In contrast with ELF basins, bonding NLMOs are defined for the whole molecular space, although they display negligible values outside their particular bond regions. Thus, due to the formally fuzzy nature of these molecular orbitals, the atomic contributions for each bond can be integrated using, exclu-

sively, the QTAIM grid. Standard QTAIM programs, as the AIM-PAC package,<sup>[29]</sup> use Gaussian quadrature techniques for integrating properties within QTAIM atomic basins. Therefore, for the  $\text{NLMO} \cap \text{QTAIM}$  scheme, Gaussian quadrature integration is performed, within each QTAIM atomic basin, using the electron density associated to the bonding NLMO [ $\phi_i^{\text{loc}} \leftrightarrow \rho_i$ , eq. (8)] instead of the total electron density.

In all cases, total electron populations were recovered by  $\text{ELF} \cap \text{QTAIM}$  fragments within 0.003 au and by  $\text{NLMO} \cap \text{QTAIM}$  within 0.001 au.

The computational treatment of ELF basins is, by far, more complicated and expensive than the use of NLMOs, particularly for atoms presenting electron lone pairs.

### Computational levels

HF and DFT (B3LYP, LDA, and M06) monodeterminantal methods were used to fully optimize closed-shell hydrogen compounds of the second and third periods (omitting noble gases). 6-31G(d,p), 6-311++(2d,2p) 6d, and aug-cc-pVTZ basis sets were used with HF and B3LYP methods to check the basis set size effect, while only the second one [6-311++(2d,2p) 6d] was used with LDA and M06 methods.

All calculations were carried out using the Gaussian 09 program.<sup>[30]</sup> Besides the software described in the previous section, the AIM-PAC package of programs<sup>[29]</sup> was also used for the analysis of the electron density.

Approximations shown in eqs. (7) and (9) are fulfilled within 0.002 au ( $\text{ELF} \cap \text{QTAIM}$ ) and 0.109 au ( $\text{NLMO} \cap \text{QTAIM}$ ), respectively.

## Results and Discussion

### Analysis of the $g_{AH}$ index

Regardless of the variety of  $g_{AH}$  values obtained from both schemes and using different computational levels (Tables 1 and 2), we highlight the presence of common general trends and that the relative dispersion is only of relevance for those atoms whose electronegativity is very close to that of H (C and S). Thus,  $g_{AH}$  basically follows the expected patterns for electronegativity in the periodic table: increases across both periods and decreases when we go down in a group (Fig. 2). As exceptions, we find that  $g_{NaH}$  and  $g_{MgH}$  are slightly bigger than  $g_{LiH}$  and  $g_{BeH_2}$  and that, in DFT calculations (excepting M06),  $g_{NaH} > g_{MgH}$ .

We find that, in general,  $g_{AH}$  values obtained with DFT methods are more positive than those obtained at HF levels. The only exceptions are those chemical elements whose  $g_{AH}$  is clearly positive: N, O, F, and Cl. Regarding the basis set size, it affects similarly to  $\text{ELF} \cap \text{QTAIM}$  and  $\text{NLMO} \cap \text{QTAIM}$  schemes. However, this effect does not follow any clear trend.

Looking at the discrepancies arising from ELF and NLMO methodologies, we observe:

- In all the cases, NLMOs enhance, with regard to ELF, the part of the BED taken by A (Fig. 2). This trend is especially noticeable in nonmetal elements, while this difference does not reach 0.07 in metals.

<sup>††</sup>The integration of  $\rho(\mathbf{r})$  in each region was carried out with a multilevel refinement. This is, when the value of  $\rho$  (in au) at a point is in the range (0.1,0.5], (0.5,1.0] or (1.0,  $\infty$ ), its value is averaged calculating it in 27, 125, or 343 points homogeneously distributed in the volume associated to the original point. Points where  $\rho(\mathbf{r}) < 0.1$  au remain unchanged.



**Table 1.** Value of the  $g_{AH}$  function for second and third period elements at different levels of calculations obtained throughout the ELF  $\cap$  QTAIM scheme.

	HF			B3LYP			LDA	M06		
A	Bs1	Bs2	Bs3	Bs1	Bs2	Bs3	Bs2	Bs2	$\bar{g}_{AH}$	SD
Li	-0.92	-0.92	-0.93	-0.91	-0.90	-0.90	-0.89	-0.91	-0.91	0.01
Be	-0.89	-0.88	-0.88	-0.87	-0.85	-0.84	-0.83	-0.86	-0.86	0.02
B	-0.73	-0.72	-0.73	-0.67	-0.63	-0.64	-0.55	-0.63	-0.66	0.06
C	-0.07	-0.05	-0.05	-0.03	-0.02	-0.02	0.04	-0.02	-0.03	0.03
N	0.36	0.33	0.36	0.32	0.29	0.31	0.32	0.29	0.32	0.02
O	0.55	0.57	0.59	0.47	0.47	0.49	0.49	0.49	0.51	0.05
F	0.67	0.70	0.72	0.57	0.60	0.62	0.61	0.64	0.64	0.05
Na	-0.85	-0.85	-0.86	-0.78	-0.75	-0.76	-0.72	-0.82	-0.80	0.05
Mg	-0.84	-0.83	-0.84	-0.78	-0.77	-0.78	-0.73	-0.78	-0.79	0.03
Al	-0.81	-0.80	-0.82	-0.76	-0.75	-0.76	-0.71	-0.75	-0.77	0.04
Si	-0.73	-0.74	-0.76	-0.69	-0.66	-0.69	-0.60	-0.66	-0.69	0.05
P	-0.64	-0.58	-0.64	-0.56	-0.47	-0.53	-0.39	-0.48	-0.54	0.08
S	-0.33	-0.22	-0.37	-0.15	-0.17	-0.12	-0.10	-0.20	-0.21	0.09
Cl	0.12	0.10	0.22	0.10	0.04	0.14	0.08	0.03	0.11	0.06

Bs1, Bs2 and Bs3 are 6-31G(d,p), 6-311++(2d,2p)6d, and aug-cc-pVTZ, respectively. Averaged value ( $\bar{g}_{AH}$ ) and standard deviation (SD) are also shown.

- $N_{AB}^{AUB}$  values obtained through NLMO  $\cap$  QTAIM are much closer to two electrons (from 1.89 to 2.00 au) than the corresponding ELF ones (from 1.24 to 1.99 au). Thus, results obtained using NLMOs should better resemble the classical picture of the chemical bond.

We find of great importance the fact that both ELF and NLMOs partitions of the electron density (despite of their different nature—disjoint vs. fuzzy) provide so similar trends for the evolution of the  $g_{AH}$  and, consequently, of the BED distribution across the periodic table. This is, therefore, a good example where two different points of view about chemical structure provide analogous results.

### Electronegativities versus $g_{AH}$

The  $g_{AH}$  index exhibits a nice “S” shape (Fig. 3) with the three scales here considered (Pauling’s, orbital-based Mulliken’s and Allred–Rochow’s). Among the three, Allred–Rochow’s scale correlate best with the bond-charge asymmetry measure pro-

vided by  $g_{AH}$ . Moreover, we also note that the “S” shape exhibited by  $g_{AH}$  versus  $\chi_{AH}$  plots agrees to the Allred’s statement: “For small electronegativity differences of the bonded atoms, the ionic character increases steadily with increasing electronegativity difference. However, if  $(\chi_A - \chi_B)$  is large, a further increases in the magnitude of  $(\chi_A - \chi_B)$  will not greatly change the ionic character.”<sup>[10]</sup> Regarding our scheme,  $g_{AB}$  replaces what Allred called “ionic character” in the previous sentence.

Our  $g_{AH}$  values were also compared to the Weinhold and Landis’ ionicity parameter at the B3LYP/6-311++(2d,2p) 6d level of theory (Fig. 4). Both  $g_{AH}$  and  $i_{AH}$  predict a similar behavior for the hydrogen-containing compounds for the more electronegative atoms. In contrast,  $i_{AH}$  values are more sensitive than  $g_{AH}$  ones to metal variation along the hydride series. This result for  $g_{AH}$  lies on the weak electron density attractor ability of the H nucleus. Because of that, when confronting hydrogen to more electropositive atoms, its basin easily gets swamped, which results in small variation in the  $g_{AH}$  values.

**Table 2.** Same as Supporting Information Table 6 for the NLMO  $\cap$  QTAIM scheme.

	HF			B3LYP			LDA	M06		
A	Bs1	Bs2	Bs3	Bs1	Bs2	Bs3	Bs2	Bs2	$\bar{g}_{AH}$	SD
Li	-0.90	-0.90	-0.90	-0.88	-0.88	-0.88	-0.87	-0.89	-0.89	0.01
Be	-0.86	-0.85	-0.85	-0.84	-0.82	-0.82	-0.80	-0.83	-0.83	0.02
B	-0.70	-0.68	-0.69	-0.63	-0.59	-0.60	-0.52	-0.59	-0.63	0.06
C	-0.03	-0.01	-0.01	0.02	0.02	0.03	0.08	0.02	0.02	0.03
N	0.41	0.40	0.42	0.39	0.37	0.39	0.40	0.38	0.40	0.02
O	0.65	0.66	0.68	0.60	0.60	0.61	0.62	0.62	0.63	0.03
F	0.78	0.80	0.81	0.72	0.75	0.76	0.76	0.77	0.77	0.03
Na	-0.80	-0.80	-0.80	-0.71	-0.69	-0.71	-0.66	-0.77	-0.74	0.05
Mg	-0.79	-0.79	-0.79	-0.74	-0.73	-0.73	-0.69	-0.74	-0.75	0.04
Al	-0.77	-0.77	-0.78	-0.72	-0.71	-0.72	-0.67	-0.72	-0.73	0.04
Si	-0.72	-0.70	-0.72	-0.65	-0.62	-0.64	-0.56	-0.62	-0.65	0.05
P	-0.52	-0.48	-0.54	-0.43	-0.36	-0.42	-0.27	-0.37	-0.42	0.08
S	-0.14	-0.04	-0.19	0.03	0.03	0.05	0.10	0.02	-0.02	0.09
Cl	0.30	0.30	0.36	0.30	0.29	0.34	0.34	0.30	0.32	0.02

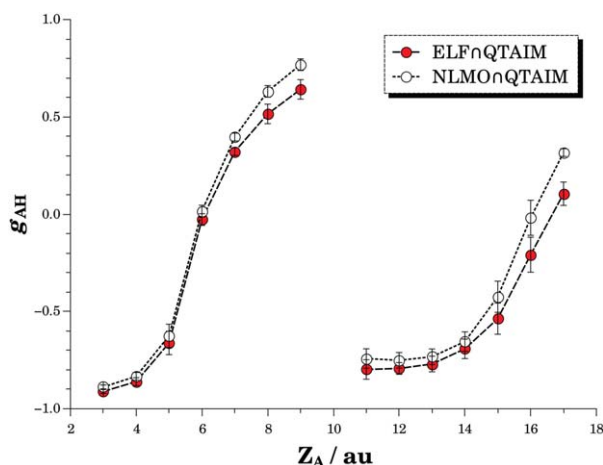


Figure 2. Averaged values of  $g_{\text{AH}}$  obtained from ELF  $\cap$ QTAIM and NLMO  $\cap$ QTAIM schemes for the elements here studied (represented by their atomic number,  $Z_{\text{A}}$ ).

### BED splitting in A–B bonds

In the previous section,  $\chi_{\text{A}}^{\text{H}}$  values were confirmed to be actually related to  $g_{\text{AH}}$  ones. Thus, as  $g_{\text{AH}}$  exhibits the properties ascribed to the electronegativity, it is tempting to explore the possibilities associated to this index. One question easily arises: “Could  $g_{\text{AH}}$  and  $g_{\text{BH}}$  indices provide any information about how the A–B BED is split atomically?” In plain English, can we state that “if  $g_{\text{AH}} > g_{\text{BH}}$ , then  $g_{\text{AB}} > 0$ ”?

It is straightforward that  $g_{\text{AB}} \neq g_{\text{AH}} - g_{\text{BH}}$ , due to the fact that, by definition,  $g_{\text{AB}}$  is contained within the  $[-1, +1]$  interval, whereas the difference is in  $[-2, +2]$ . However, both  $g_{\text{AH}}$  and  $g_{\text{BH}}$  measure the ability of A (and B) to attract to itself the BED of a A–H (B–H) bond. Then, if the chemical nature of an A–B bond is alike A–H and B–H bonds and if  $g_{\text{AB}}$  increases monotonically with  $\chi_{\text{A}}^{\text{B}}$ , a qualitative prediction about the  $g_{\text{AB}}$  sign can be obtained from them, as illustrated in Table 3. Therefore,  $g_{\text{AH}}$  values could be considered as a kind of “electronegativity” scale based on hydrogen compounds, as they also indicate which atom of a certain bond acquires more BED.

### Effect of the hybridization on $g_{\text{AH}}$

As usual electronegativity scales just contain one value for each chemical element, transferability could be expected as a desirable property for  $\chi$ . When relating electronegativity to BED atomic partitioning, we realize that complete transferability is an unreachable limit, as it was demonstrated<sup>[31]</sup> by extending the Hohenberg–Kohn theorem<sup>[32]</sup> to open systems.<sup>[33]</sup> Moreover, electronegativity also depends on the chemical environment. In fact, it is well known that  $\chi_{\text{C}(\text{sp})} > \chi_{\text{C}(\text{sp}^2)} > \chi_{\text{C}(\text{sp}^3)}$ . We think it can be of interest to check how  $g_{\text{AH}}$  behaves when dealing with an atom in different hybridizations. Ethane, ethene, and ethine are typically ascribed in bibliography as clear examples of  $\text{sp}^3$ ,  $\text{sp}^2$ , and  $\text{sp}$  hybridization for C atom, respectively. For a B3LYP/6-

311++(2d,2p) 6d level of calculation,  $g_{\text{CH}}$  was obtained from the corresponding C–H bonds. As expected,  $g_{\text{CH}}$  increases as the s character does. Thus, its values are  $-0.02$ ,  $0.06$ , and  $0.24$  for ethane, ethene, and ethine, respectively, using the ELF  $\cap$ QTAIM scheme ( $0.1$ ,  $0.5$ , and  $0.18$  with NLMO  $\cap$ QTAIM).

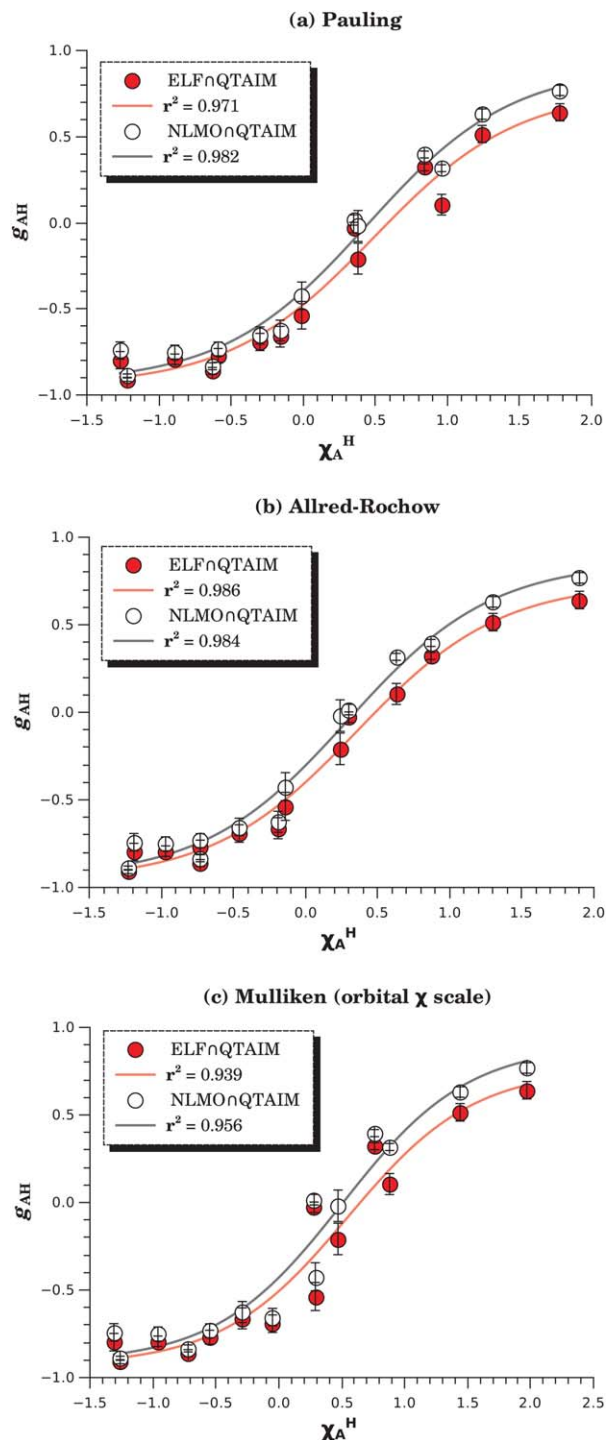


Figure 3. Plots of  $g_{\text{AH}}$  versus electronegativity. A sigmoid function, defined by  $g_{\text{AH}} = a \cdot \tanh(b + \chi_{\text{A}}^{\text{H}}) + c$ , was fitted to data points. Mulliken's scale values are based on orbital electronegativities and taken from the Bergmann and Hinze's review.<sup>[17]</sup> [Color figure can be viewed in the online issue, which is available at [wileyonlinelibrary.com](http://wileyonlinelibrary.com).]

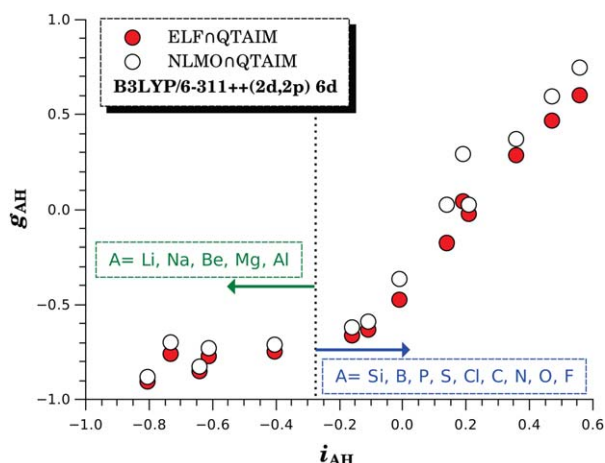


Figure 4. Plot of  $g_{AH}$  versus  $i_{AH}$ . [Color figure can be viewed in the online issue, which is available at [wileyonlinelibrary.com](http://wileyonlinelibrary.com).]

## Conclusions

Two computational schemes based, respectively, on splitting ELF basins and NLMOs, with QTAIM atomic separatrixes, are proposed to evaluate how the BED is atomically divided in hydrogen compounds. Both schemes provide the same chemical picture of the system, despite using partitions of different nature (fuzzy vs. disjoint) to describe two-electron regions in molecules. We note that the NLMO  $\cap$  QTAIM scheme is much less expensive in terms of computational efforts.

Both ELF  $\cap$  QTAIM and NLMO  $\cap$  QTAIM schemes were used to compute values for the  $g_{AH}$  index, which measures the amount of A—H BED taken by atom A. This function follows the expected patterns for electronegativity across the periodic table. Moreover, it is a monotonically increasing function with regard to the A-RE. This indicates that A-RE values are the most concordant, among the common electronegativity scales here considered, to describe the A—H BED splitting predicted by the schemes here proposed. Furthermore, pairs of  $g_{AH}$  and  $g_{BH}$  values allow to predict which atom attracts more BED in a A—B bond of similar chemical nature. Finally,  $g_{CH}$  values computed for compounds with different C hybridization increase as the s character does.

Table 3. Different  $g_{AB}$  values from ELF  $\cap$  QTAIM and NLMO  $\cap$  QTAIM schemes.

Molecule	A	B	$\chi_A^B$	ELF		NLMO	
				$g_{AB}$	$g_{AH}^{BH}$	$g_{AB}$	$g_{AH}^{BH}$
HBe—F	Be	F	−2.63	−0.91	−1.45	−0.93	−1.57
H <sub>2</sub> B—F	B	F	−2.09	−0.86	−1.23	−0.87	−1.34
H <sub>3</sub> C—F	C	F	−1.60	−0.62	−0.62	−0.65	−0.73
H <sub>3</sub> C—OH	C	O	−1.00	−0.53	−0.49	−0.54	−0.58
H <sub>3</sub> C—NH <sub>2</sub>	C	N	−0.57	−0.33	−0.31	−0.32	−0.35
H <sub>2</sub> N—OH	N	O	−0.43	−0.15	−0.18	−0.21	−0.23
H <sub>3</sub> C—SH	C	S	0.06	0.09	0.15	−0.07	−0.00
H <sub>3</sub> C—PH <sub>2</sub>	C	P	0.44	0.40	0.45	0.30	0.39
H <sub>3</sub> C—SiH <sub>3</sub>	C	Si	0.76	0.70	0.64	0.64	0.64

$\chi_A^B$  from Allred—Rochow scale and  $g_{AH}^{BH} = (g_{AH} - g_{BH})$  difference are also shown. All these values were obtained from B3LYP/6-311++(2d,2p) 6d electron densities.

Although a pair of  $g_{AH}$  and  $g_{BH}$  values cannot be used to quantitatively predict the BED distribution of a certain A—B bond, we observe that  $g_{AH}$  values exhibit properties typically ascribed to electronegativities and, therefore, they could be considered as another electronegativity scale based on hydrogen compounds.

## Acknowledgments

D. F-C. thanks Spanish Ministry of Education for an FPU fellowship.

**Keywords:** electronegativity • electron localization function • QTAIM • natural localized molecular orbital • atomic partition

How to cite this article: D. Ferro-Costas, I. Pérez-Juste, R. A. Mosquera. *J. Comput. Chem.* **2014**, *35*, 978–985. DOI: 10.1002/jcc.23574

Additional Supporting Information may be found in the online version of this article.

- [1] A. D. McNaught, A. Wilkinson, IUPAC. Compendium of Chemical Terminology, 2nd ed. (the "Gold Book"); Blackwell Scientific Publications: Oxford, **1997**.
- [2] R. Chang, Chemistry, 10th ed.; McGraw-Hill, New York, **2010**.
- [3] R. H. Petrucci, F. G. Herring, J. D. Madura, C. Bissonnette, General Chemistry: Principles and Modern Applications, 10th ed.; Pearson Prentice Hall, Toronto, **2011**.
- [4] L. Pauling, *J. Am. Chem. Soc.* **1932**, *54*, 3570.
- [5] W. B. Jensen, *J. Chem. Edu.* **2012**, *89*, 94.
- [6] W. H. Rodebush, *J. Chem. Edu.* **1925**, *2*, 381.
- [7] W. H. Rodebush, *Science*, **1924**, *59*, 430.
- [8] G. H. Cartledge, *J. Am. Chem. Soc.* **1928**, *50*, 2855.
- [9] M. L. Huggins, *J. Am. Chem. Soc.* **1953**, *75*, 4123.
- [10] A. L. Allred, *J. Inorg. Nucl. Chem.* **1961**, *17*, 215.
- [11] R. S. Mulliken, *J. Chem. Phys.* **1934**, *2*, 782.
- [12] A. L. Allred, E. G. Rochow, *J. Inorg. Nucl. Chem.* **1958**, *5*, 264.
- [13] P. Geerlings, F. De Proft, W. Langenaeker, *Chem. Rev.* **2003**, *103*, 1793.
- [14] R. G. Parr, R. A. Donnelly, M. Levy, W. E. Palke, *J. Chem. Phys.* **1978**, *68*, 3801.
- [15] R. P. Iczkowski, J. L. Margrave, *J. Am. Chem. Soc.* **1961**, *83*, 3547.
- [16] J. Hinze, M. A. Whitehead, and H. H. Jaffé, *J. Am. Chem. Soc.* **1963**, *85*, 148.
- [17] D. Bergmann, J. Hinze, *Angew. Chem. Int. Ed. Engl.* **1996**, *35*, 150.
- [18] A. D. Becke, K. E. Edgecombe, *J. Chem. Phys.* **1990**, *92*, 5397.
- [19] A. Savin, R. Nesper, S. Wengert, T. F. Fässler, *Angew. Chem. Int. Ed. Engl.* **1997**, *36*, 1808.
- [20] R. F. W. Bader, *Atoms in Molecules: A Quantum Theory*; Clarendon Press: Oxford, **1995**.
- [21] R. F. W. Bader, *Chem. Rev.* **1991**, *91*, 893.
- [22] D. Ferro-Costas, R. A. Mosquera, *J. Chem. Theory Comput.* **2013**, *9*, 4816.
- [23] A. E. Reed, F. Weinhold, *J. Chem. Phys.* **1985**, *83*, 1736.
- [24] A. E. Reed, L. A. Curtiss, F. Weinhold, *Chem. Rev.* **1988**, *88*, 899.
- [25] F. Weinhold, C. Landis, *Valency and Bonding. A Natural Bond Orbital Donor-Acceptor Perspective*; Cambridge University Press, New York, **2005**.
- [26] R. F. W. Bader, *Pure Appl. Chem.* **1988**, *60*, 145.
- [27] W. Tang, E. Sanville, G. Henkelman, *J. Phys.: Condens. Matter* **2009**, *21*, 084204.
- [28] T. Lu, F. Chen, *J. Comput. Chem.* **2012**, *33*, 580.
- [29] R. Biegler-Knig, R. Bader, T.-H. Tang, *J. Comput. Chem.* **1982**, *13*, 317.
- [30] M. J. Frisch, G. W. Trucks, H. B. Schlegel, G. E. Scuseria, M. A. Robb, J. R. Cheeseman, G. Scalmani, V. Barone, B. Mennucci, G. A. Petersson, H. Nakatsuji, M. Caricato, X. Li, H. P. Hratchian, A. F. Izmaylov, J. Bloino, G. Zheng, J. L. Sonnenberg, M. Hada, M. Ehara, K. Toyota, R. Fukuda, J. Hasegawa, M. Ishida, T. Nakajima, Y. Honda, O. Kitao, H. Nakai, T. Vreven,



J. A. Montgomery, Jr., J. E. Peralta, F. Ogliaro, M. Bearpark, J. J. Heyd, E. Brothers, K. N. Kudin, V. N. Staroverov, R. Kobayashi, J. Normand, K. Raghavachari, A. Rendell, J. C. Burant, S. S. Iyengar, J. Tomasi, M. Cossi, N. Rega, J. M. Millam, M. Klene, J. E. Knox, J. B. Cross, V. Bakken, C. Adamo, J. Jaramillo, R. Gomperts, R. E. Stratmann, O. Yazyev, A. J. Austin, R. Cammi, C. Pomelli, J. W. Ochterski, R. L. Martin, K. Morokuma, V. G. Zakrzewski, G. A. Voth, P. Salvador, J. J. Dannenberg, S. Dapprich, A. D. Daniels, Ö. Farkas, J. B. Foresman, J. V. Ortiz, J. Cioslowski, D. J. Fox, *Gaussian 09 Revision A.02*. Gaussian, Inc., Wallingford CT, **2009**.

- [31] R. F. W. Bader, P. Becker, *Chem. Phys. Lett.* **1988**, 148, 452.  
[32] P. Hohenberg, W. Kohn, *Phys. Rev.* **1964**, 136, B864.  
[33] J. Riess, W. Münch, *Theor. Chim. Acta* **1981**, 58, 295.

---

Received: 18 December 2013

Revised: 13 February 2014

Accepted: 17 February 2014

Published online on 10 March 2014